Chapter 2: Materials and Methods

2.1 Introduction

This chapter provides a detailed account of the steps taken to achieve the objectives. It commences by outlining the design procedure, melting and casting, thermomechanical processing employed for the development of austenitic steel, austenitic steel with reinforcement and austenite based duplex steel. The austenite based duplex steel has also undergone electropulsing treatment with a high current density to modify the microstructure, and various characterization techniques are adopted to correlate the microstructure and mechanical properties.

2.2 Composition design

Three steel compositions are designed using ThermoCalc software (TCFE database version 2022a) to get austenite, austenite + TiC composite and austenite + B2. The designed compositions (Fe-18Mn-6.5Al-0.75C, Fe-18Mn-6.5Al-1.25C-2.5Ti, and Fe-18Mn-10Al-1C-6Ni (all by mass%), respectively) of the steels are designated as P1, P2, and P3, which are presented in Table 2.1.

Table 2.1: Designed compositions (all by mass %).

Designation	Composition (mass %)						Steel type
	Mn	Al	C	Ni	Ti	Fe	
P1	18	6.5	0.75	0	0	Rest	Austenitic
P2	18	6.5	1.25	0	2.5	Rest	Austenite + TiC
P3	18	10	1	6	0	Rest	Austenite based duplex

The first composition (P1) is tailored to get a fully austenitic microstructure to obtain high ductility. The second composition (P2) is designed by adding 2.5 mass % of titanium and an additional 0.5 mass % of carbon to the P1 composition to achieve a 5 vol.% of in-situ TiC-reinforced austenitic low-density steel with an enhanced elastic modulus. The third composition (P3) is developed to obtain austenite + B2 by adding 6% nickel and an additional 3.5 mass % of Al, 0.25 mass % of C to P1 composition to achieve high strength, resulting in an austenite-based duplex low-density steel. Phase diagrams of P1, P2, and P3 are plotted with temperature versus varying amount of Al (mass %) using ThermoCalc software while keeping 18 % Mn for all PD1, PD3 compositions, but 0.75C for P1, and 1C-6Ni for P3 as constants, respectively. Phase fraction versus Temperature diagram is drawn for P2 composition.

2.3 Alloy making

To make the designed compositions, raw materials (high-carbon steel, high-carbon ferromanganese powder, pure electrolytic manganese, aluminum, nickel and titanium) are procured from Mishra Dhatu Nigam Limited, Hyderabad, India. A 2 kg mix of raw materials for P1 composition are prepared with the required proportions by using mass balance equations. The mix (P1) of dried high-carbon steel, aluminium, are melted in a vacuum induction furnace (made by Inductotherm India Pvt Ltd., 15 kW, 10 kHz), at a temperature of 1600°C, with a pressure of 10^{-4} mbar, in a zirconia crucible. After complete melting, the melt is stirred by induction for 10 min to get a homogeneous mix. The temperature is reduced to 1560°C and the vacuum was broken. Argon gas is purged and a pressure of 600-700 mbar is maintained. High carbon ferromanganese powder and electrolytic manganese are added to the melt maintained at 1560°C to reduce the vaporization of Mn. After Mn/Fe-Mn are completely melted (~ 5 min), the melt is

homogenized through induction stirring, for ~3 min. The homogenised melt is cast into a plate of 150 mm × 100 mm × 15 mm in a copper mould. Figure 2.1 shows the vacuum induction melting furnace located at the Advanced Steel Research Centre for Iron and Steel (ARCIS) within the Department of Metallurgical Engineering, IIT BHU, Varanasi. Figure 2.2 (a) shows the copper mould used for casting. Figure 2.2 (b) illustrates the dimensions of one half of the copper mold. Figure 2.2 (c) displays an image of the produced as-cast plate.

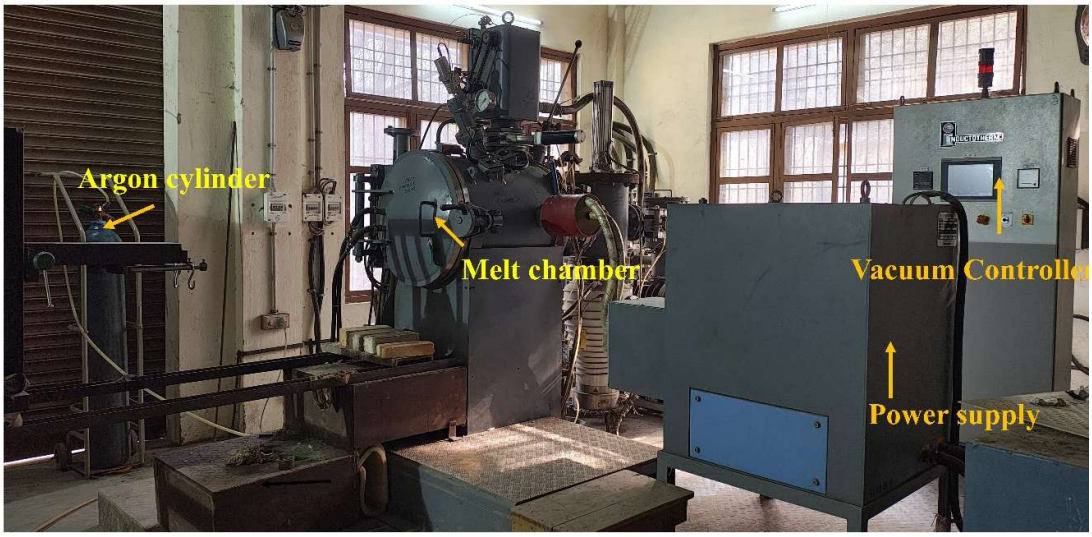

Figure 2.1: Vacuum induction melting furnace facility at ARCIS centre.

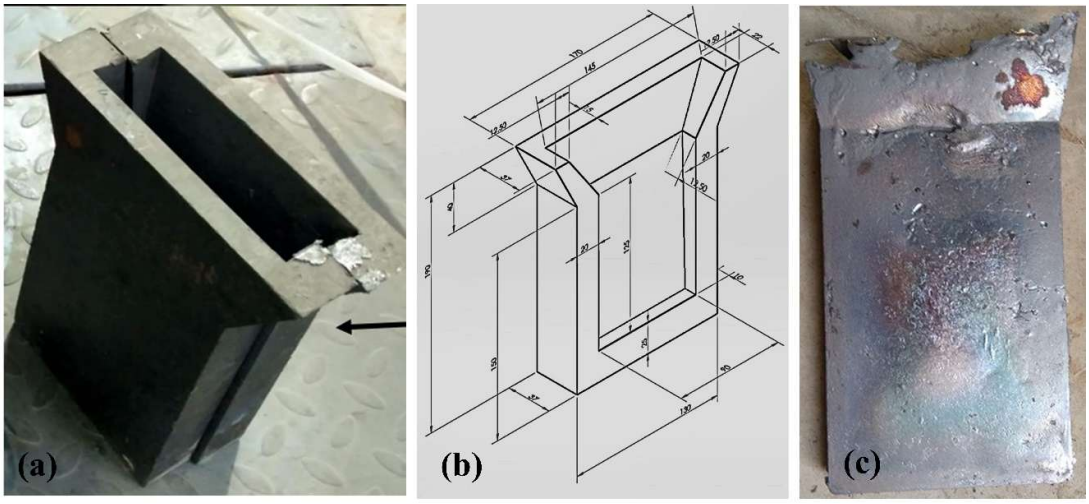

Figure 2.2: (a) copper mould (b) dimensions of half side of copper mould (c) cast plate.

Compositions of P2 and P3 are also melted with their respective alloying elements and Mn/Fe-Mn are added in the same sequence as of P1 and cast.

2.3.1 Thermomechanical & Heat treatment processes for P1&P2

Rectangular bars of 100 mm × 15 mm × 12 mm dimensions are sectioned from the cast plate using a wire-cut Electrical Discharge Machine (EDM). These bars are initially thermomechanically processed (homogenized at 1080°C for 1 h to get uniform composition, followed by hot rolling with a 75% reduction in thickness to break the cast structure and to get the required dimension), as illustrated in Figure 2.3 (a). The finish rolling temperature is maintained at 950°C, and the rolled materials are air-cooled. These rolled alloys of P1, P2 are designated as PD1 and PD2. Subsequently, both PD1 and PD2 alloys are solutionized at 950°C for 30 min to dissolve the precipitates, followed by water quenching. The solutionized PD1 and PD2 materials are labeled as PD1-S and PD2-S, respectively. The PD1-S samples are then rolled at room temperature with 80% reduction in thickness to introduce the maximum possible dislocation density. The cold rolled PD1-S materials are designated as PD1-SC. The PD1-SC samples are annealed at 900°C for 2 min and water quenched. This thermal cycle of annealing for short time is repeated twice. The repeatedly annealed samples are designated as PD1-SCR. Cold rolling followed by repeated annealing treatment for PD1-S is illustrated in Figure 2.3 (b).

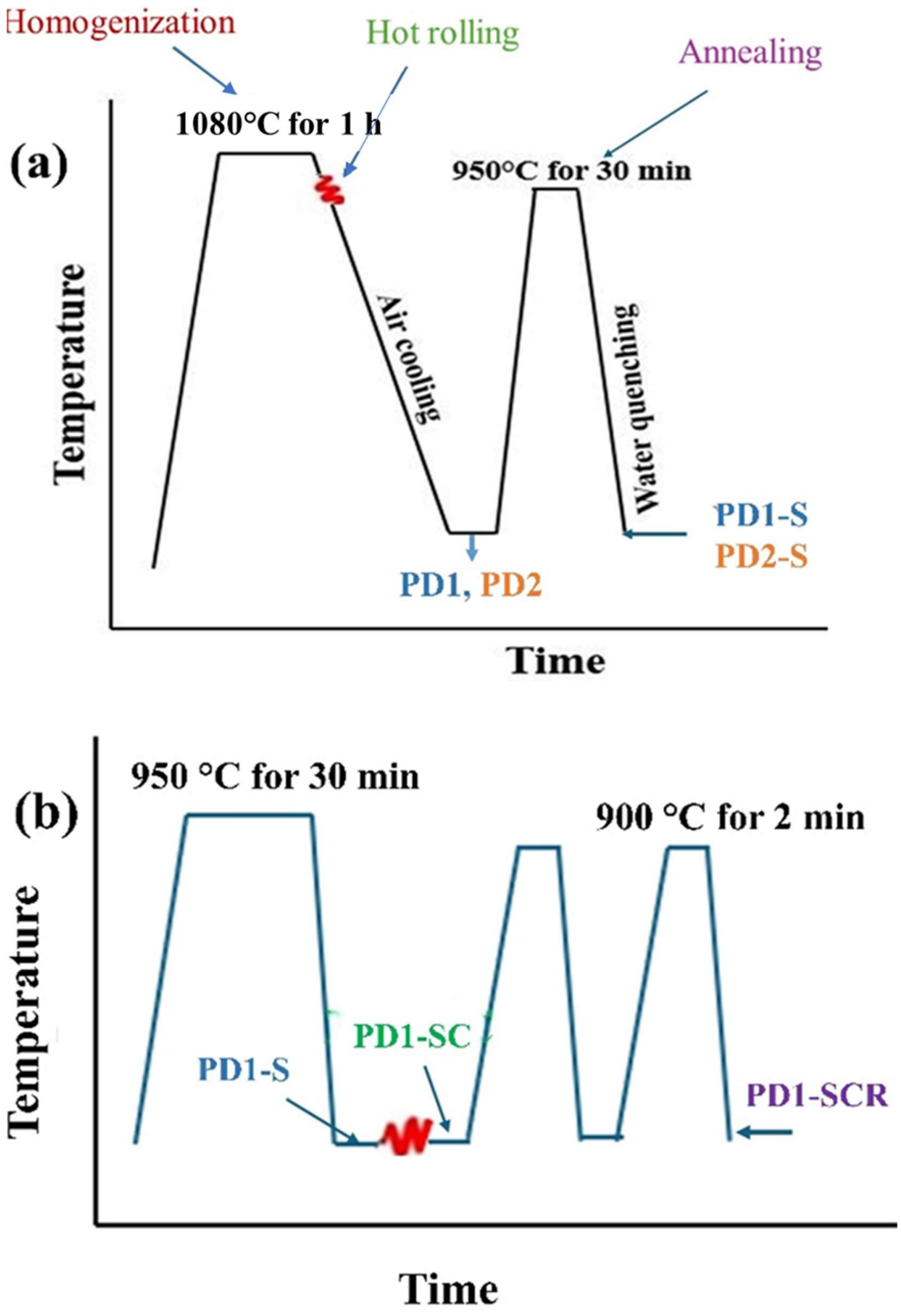

Figure 2.3: Schematic representation of (a)Thermomechanical processing followed by annealing treatment for P1, P2 (b) cold rolling followed by repeated annealing treatment of PD1-S.

2.3.2 Thermomechanical & Heat treatment processes for P3

Rectangular bars of P3 of 100 mm × 15 mm × 12 mm dimensions are cut from the cast plate using a wire-cut Electrical discharge machine (EDM). The bars are thermomechanically treated by homogenizing at 1200°C for 1 h, followed by hot rolling for a 75% reduction in thickness to break the cast structure and water quenching as shown in Figure 2.4. Hot rolling is performed at 1150 °C for reduction of 1mm/pass for 7 times with intermittent heating. After, the rolled material is further thinned down by reducing 2mm/pass. The finish rolling temperature is 950 °C. Hot rolled sample is immediately quenched in water to room temperature to retain the maximum achievable dislocation density and to avoid undesirable precipitation. The hot rolled and water-quenched material

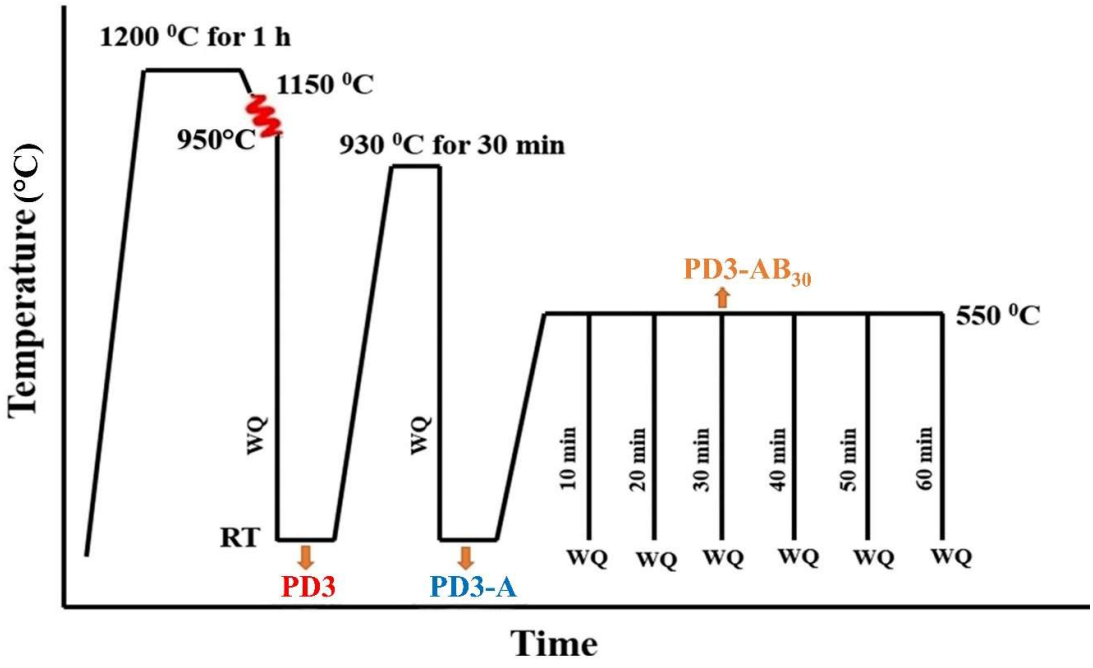

Figure 2.4: Schematic representation of thermomechanical process followed by annealing and aging treatments.

is designated as PD3. The PD3 samples are subjected to annealing at 930°C for 30 min to get additional B2 precipitation, followed by water quenching. The annealed PD3 alloy is referred to as PD3-A. Further, PD3-A samples are aged at 550°C for various periods of 10, 20,30 40, 50, and 60 min to obtain different proportions of kappa carbides, followed by water quenching. The aged materials are designated as PD3-AB_t, where t stands for 10,20,30,40,50,60, respectively.

2.3.3 Composition analysis

The hot rolled samples of PD1, PD2 and PD3 are analyzed for carbon content in a LECO CS744 analyzer. The remaining elements are analyzed by inductively coupled plasma-optical emission spectroscopy. The compositions of the rolled alloys (by mass %) are given in Table 2.2. The densities of PD1, PD2 and PD3 samples are measured based on Archimedes' principle. Initially, the dry weight of the sample is taken in air as W_A in g. The sample did not have any open pores. After boiling the sample in water, the sample and water combination was cooled to room temperature. The sample is suspended in cold water and the suspended weight is recorded as W_S in g. The ratio of W_A and W_A-W_S is determined. Dry density is determined by multiplying the ratio of W_A and W_A-W_S with the density of liquid (water in this case).

Table 2.2: Analyzed compositions of PD1, PD2 and PD3.

Material designation	Composition (mass %)						Steel type
	Mn	Al	C	Ni	Ti	Fe	
PD1	18.93	6.20	0.76	0.05	0	Rest	Austenitic
PD2	19.85	6.58	1.15	0.05	2.38	Rest	Austenite + TiC
PD3	18.95	10.51	1.04	5.88	0	Rest	Austenite based duplex

2.3.4 Electropulsing Treatment

The PD3-A and PD3-AB_{30} materials are further machined to dimensions of 65 mm × 12 mm × 2 mm strips, as shown in Figure 2.5 (a). The strip samples are electropulsed using a setup given in Figure 2.5 (b). The setup consists of input power of 415 V, 50 Hz, 3φ power supply, capacitor charging power supply (CCPS), capacitor bank with a protection circuit, a load cell with copper electrodes, rogowski coil and a display device of cathode ray oscilloscope (CRO). CCPS receives 3φ input power of 415 V AC supply at the rate of 2A. voltage is stepped up using a step-up transformer to the required level (0-16kV), utilizing a control circuit. The CCPS charges the capacitor bank at the current rate of 200mA DC, and the bank stores the power at the rate of 2.8kJ/sec to maximum energy of 39 kJ. The capacitor bank consists of 14 number of parallelly connected capacitors with 14 μF capacitance of each, and total capacitance of 196 μF. Main power supply is switched off. Then a trigger pulse provided by the trigger generator actuates the spark gap which closes the spark gap switch that sends high power to the load cell/sample. Current is measured through a rogowski coil, with the help of CRO. The output current is displayed as a damped oscillation shown in Figure 2.5 (c) and Figure 2.5 (d) for PD3-A, PD3-AB_{30} samples, respectively. Only one pulse is given to both PD3-A and PD3-AB_{30} samples. The maximum current densities derived from the first peak of the damped wave, are calculated to be 7.5 kA/mm², 8 kA/mm² for PD3-A and PD3-AB30, respectively. The damping of first peaks are observed at a time period of 49 μs, 52 μs, respectively, for PD3-A and PD3-AB_{30} samples. The total discharge duration is 310 μs for PD3-A and 296 μs for PD3-AB_{30}. The average current densities of both samples are calculated to be 3.9 kA/mm². A summary of the electropulsing parameters is provided in Table 2.3.

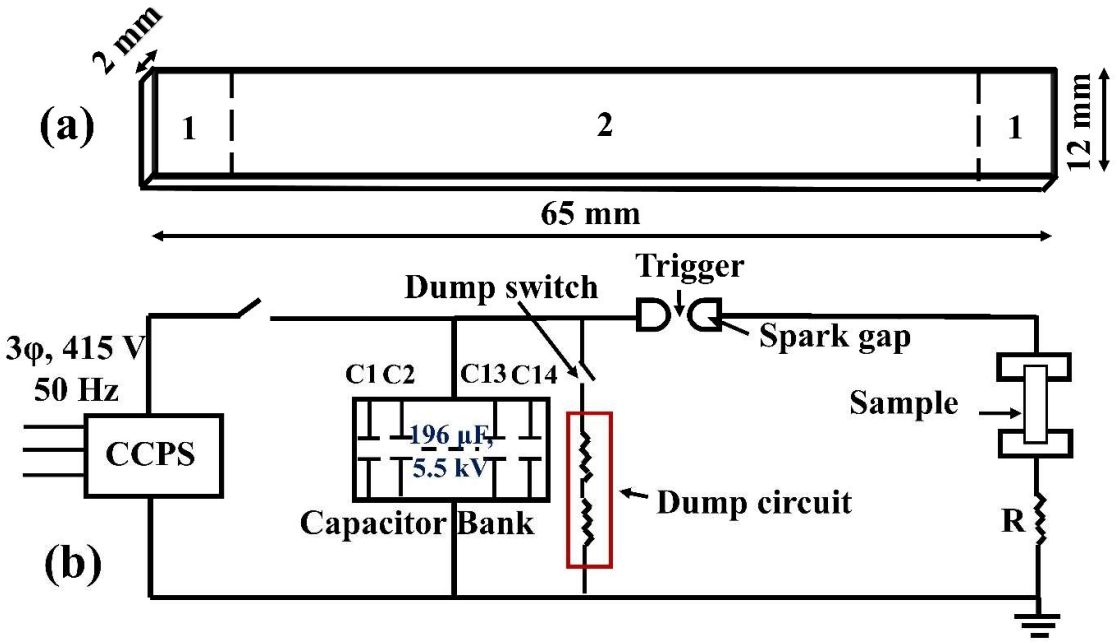
(a)
2 mm
1
2
1
12 mm
65 mm
(b)
3φ, 415 V
50 Hz
CCPS
C1 C2
C13 C14
196 μF,
5.5 kV
Capacitor Bank
Dump switch
Trigger
Spark gap
Dump circuit
Sample
R

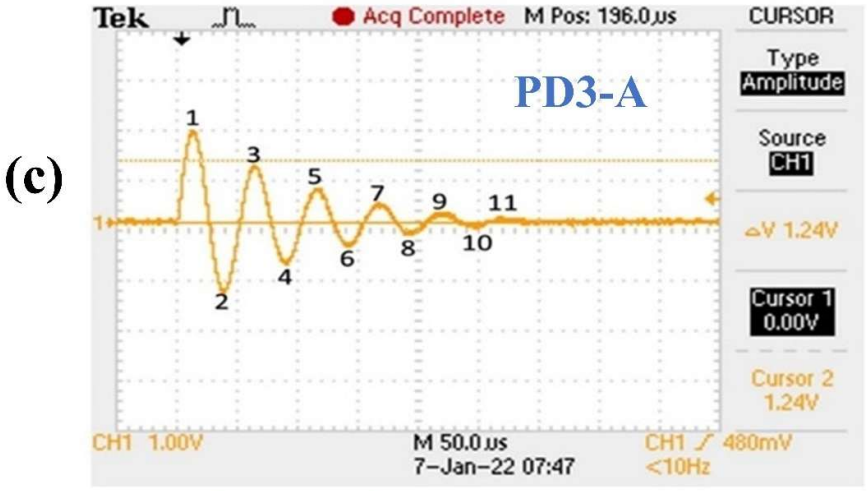
(c)
Tek
Acq Complete
M Pos: 196.0μs
CURSOR
PD3-A
Type
Amplitude
Source
CH1
ΔV 1.24V
Cursor 1
0.00V
Cursor 2
1.24V
CH1 1.00V
M 50.0μs
7-Jan-22 07:47
CH1 480mV
<10Hz

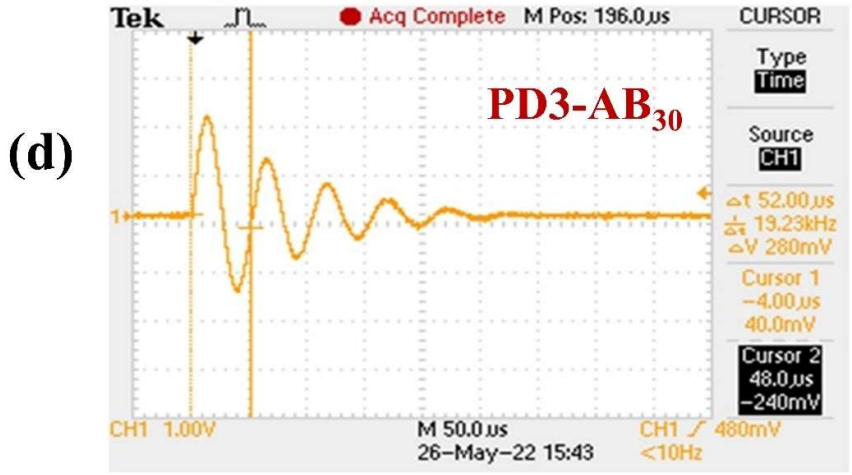
(d)
Tek
Acq Complete
M Pos: 196.0μs
CURSOR
PD3-AB30
Type
Time
Source
CH1
Δt 52.00μs
1/Δt 19.23kHz
ΔV 280mV
Cursor 1
-4.00μs
40.0mV
Cursor 2
48.0μs
-240mV
CH1 1.00V
M 50.0μs
26-May-22 15:43
CH1 480mV
<10Hz

Figure 2.5: (a) Electropulsing sample with (1) clamping region and (2) area for microstructural and tensile characterization (b) Schematic of the electropulsing (EP) setup, EP output waveform (c) for PD3-A, (d) for PD3-AB_{30} (where 1 division in waveform on y-axis is 1V, which is equivalent to 100 kA of output current. 1 division on x-axis is 50 µs).

Table 2.3: Electropulsing parameters.

Sample	Voltage (kV)	Time (1st peak) (µS)	Total time (µS)	1st peak Current density (Max.) (kA/mm^2)	Average current density (kA/mm^2)
PD3-A	5.5	49	310	7.5	3.9
PD3-AB_{30}	5.5	52	296	8	3.9

The image of the electropulsing facility available in Metallurgical Engineering department at IIT BHU is presented in Figure 2.6.

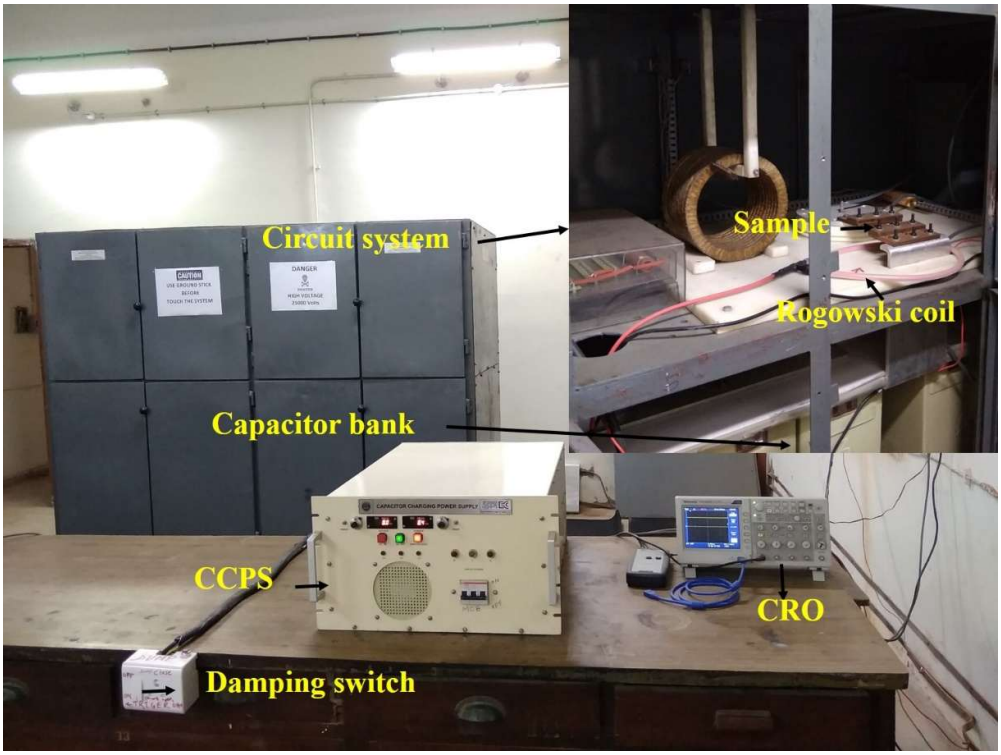

Figure 2.6: Electropulsing facility in Metallurgical Engineering department.

2.4 Microstructural characterization

2.4.1 Optical microscopy

Approx. 10 x 10 mm^2 samples are cut from the processed materials of specific compositions by EDM. The cut samples are ground using SiC abrasive papers followed by polishing on a velvet cloth by applying a suspension of fine (0.5 μm) alumina powder and water. The polished samples are etched with 5% nital solution. The etched samples are studied in a Leica DFC 295 optical microscope to observe the size, shape and size distribution of phases. The grain size of austenite, TiC, banded, globular and platelet of B2 precipitates are determined through the utilization of ImageJ software after calibration of image pixcel size to micron bar, with a consideration of 50, 50, 20, 30, and 100 number of particles, respectively. Average sizes with standard deviations are reported.

2.4.2 X-Ray Diffraction

Another set of 10 x10 mm^2 samples are cut from the processed materials of specific compositions by EDM. The samples are fine polished and scanned using Cu-Kα radiation at the operating voltage of 45 kV and current of 40 mA, in a Malvern Panalytical Empyrean model with a 3D Pixcel detector X-ray diffractometer in the angular range of 15° to 135 °, with a scanning speed of 1°/min and a step size of 0.01°. The raw XRDML files obtained from the XRD machine were analyzed using X'Pert High Score Plus software. Initially, the background is stripped, followed by conducting a peak search. Subsequently, Kα2 radiation is eliminated. The identified peaks are then fitted using Pseudo-Voigt fitting, which provided the corresponding Bragg angles, d-spacing values and area under the peak. The phases are identified by comparing the d-spacing values and corresponding Bragg angles with those listed in the ICDD PDF2 database. The volume fractions of the phases are determined by the ratio of the sum area of all the peaks of a phase (i.e. austenite or B2

phase or TiC or kappa carbide) and the total sum area of all the peaks of all the phases from the XRD pattern as shown in Equation 2.1 [104].

$$V_A = \frac{\sum_{i=1}^{n} A_\gamma}{\sum_{i=1}^{n} A_\gamma + \sum_{i=1}^{n} A_{B2}} \quad [2.1]$$

Where V_A is the volume fraction of retained austenite, A_γ and A_δ are area under XRD peaks of austenite, and B2 respectively. Similarly, the volume fractions of B2, kappa carbide, and TiC phases can be calculated by summing their respective peak areas and dividing by the total peak area summation.

Crystallite size (t_{hkl}) and lattice microstrain (e_{hkl}) are determined on the XRD peaks of austenite ((111), (200), (220) planes) in all the characterized samples and B2 ((110), (200), and (211) planes) in PD3, PD3-A and PD3-AB_{30}, PD3-AE and PD3-AB_{30}E samples, from the corrected Lorentzian (for estimation of crystallite size) and the Gaussian (for estimation of micro strain) components of integral breadth widths. The Lorentzian (β_{LSi}) and Gaussian (β_{GSi}) components of integral breadth of standard Si crystal (Table 2.4) is represented by two second order polynomial equations (Equation 2.2, Equation 2.3).

$$\beta_{LSi} = a_0 + a_1 x + a_2 x^2 \quad [2.2]$$

$$\beta_{GSi} = b_0 + b_1 x + b_2 x^2 \quad [2.3]$$

Where x is the 2θ of diffracting plane.

By using Lorentzian and gaussian components of integral breadth values for 3 peaks of (111), (220) and (311) planes of 2θ positions are solved for a_0, a_1, a_2 and b_0, b_1, b_2 variables and found out to be 0.0165, -0.000368991, 4.22 and 0.00167, -0.000431599, 0.00181, respectively. By using these constant values, a general equation for Lorentzian component of integral breadth of instrumental broadening is written as of Equation 2.4.

Instrumental broadening (Lorentzian), β_{LI} = 0.00165 + (-3.68991*10^{-4} (x) + 4.22 (x^2)) [2.4]

Similarly, for Gaussian component of integral breadth of instrumental broadening is written as of Equation 2.5.

Instrumental broadening (Gaussian), β_{GI} = 0.00167 + (-4.31599*10^{-4} (x) +0.00181 (x^2) [2.5]

The Lorentzian component of instrumental breadth β_{LI} values for the respective 2θ positions of austenite and B2 reflecting planes is obtained by putting the 2θ value in a polynomial equation (Equation 4). The corrected Lorentzian component of the integral breadth β'_L for each plane of austenite and B2 phase is separated from the respective Lorentzian component (β_L) using Equation 2.6.

$$\beta'_L = \beta_L - \beta_{LI} \quad [2.6]$$

Table 2.4: Integral breadth of standard Silicon.

Std. Si, 2θ, (°)	Gaussian Integral Breadth, β_G, (°)	Lorentzian integral Breadth, β_L, (°)
33.15	0.11579	0.10049
55.55	0.1703	0.12117
66.25	0.20427	0.11799
82.47	0.27518	0.14347
91.77	0.11321	0.12747

Similarly, instrumental breadth β_{GI} for the respective 2θ of austenite and B2 reflecting planes is obtained by putting the 2θ value in a polynomial equation (Equation 2.5). The corrected (for instrumental broadening) Gaussian component (β'_G) of the integral breadth

of a diffracting plane of a phase is extracted from the Gaussian component (β_G) using Equation 2.7.

$$\beta'^2_G = \beta^2_G - \beta^2_{GI} \quad [2.7]$$

The crystallite size (t_{hkl}) and lattice microstrain (e_{hkl}) are calculated from Equation 2.8 and Equation 2.9, respectively [105] on all planes of respective phases.

$$t_{hkl} = \frac{0.91\lambda}{\beta'_L Cos(\theta)} \quad [2.8]$$

$$e_{hkl} = \frac{\beta'_G}{4tan\theta} \quad [2.9]$$

Where 2θ is the Bragg angle and λ is the wavelength of the X-ray radiation.

The dislocation density at (*hkl*) is calculated for crystallite size and micro strain using Equation 2.10 [106], [107] from the diffraction measurement.

$$\rho_{hkl} = \frac{2\sqrt{3}\langle e^2_{hkl}\rangle^{1/2}}{D_{hkl}b} \quad [2.10]$$

Where b is the Burger vector taken for austenite as 2.56 Å.and 2.52Å for B2.

2.4.3 Scanning Electron Microscopy

The light etched optical samples are also studied in a scanning electron microscope (FEI Scios II dual beam FIB-FESEM) for the processed materials of specific compositions. The size of globular and platelet type B2 precipitates are determined on the high-resolution micrographs (taken from SEM) by using ImageJ software. B2 precipitates distribution, and morphology of phases are also determined. Additionally, the compositions of the austenite, TiC and different types of B2 are determined using energy dispersive spectroscopy (EDS). For Electron Backscattered Diffraction (EBSD) studies, 10 × 10 × 3 mm^3 samples are mounted on conducting polymer, ground, and polished using colloidal silica of 0.05 μm size. The samples are scanned using the above scanning electron microscope operating at a 20 kV accelerating voltage, 15 mm working distance, and a tilt angle of 70° with a scan

area of 100 × 100 μm², and a step size of 0.15 μm with EBSD detector. The scanned data is cleaned with a grain tolerance angle lower than 2° and a confidence index lower than 0.1 in TSL-OIM version 8 software. The cleaned data is analysed for phase fractions, grain size, high angle and low angle grain boundaries, micro texture and residual strain (kernel average misorientation (KAM) maps) in the material.

2.4.4 Transmission Electron Microscopy

A thin slice of 1 mm thickness is cut from the processed samples and mechanically ground to a thickness of 50 μm using silicon carbide abrasive papers. Subsequently, 3 mm diameter discs are punched from the foil and subjected to electrolytic polishing in a twin-jet electropolisher using a solution comprising 10 vol. % perchloric acid and 90% ethanol at 20 V and a temperature of -20°C. The electropolished samples are then examined using a Tecnai G^2 20 TWIN transmission electron microscope (TEM) operating at 200 kV for detailed microstructure. Phases are confirmed by analysing diffraction patterns. The morphology and size of kappa carbide, ferrite (K-pearlite) is measured based on the TEM bright field image using ImageJ software.

2.5 Mechanical characterization

2.5.1 Hardness Test

The hardness measurement is carried out on polished heat-treated samples of dimension 10 x10 x 2 mm^3 using the Leco LM 248 AT Vickers hardness tester at a load of 1 kgf and a dwell time of 15 seconds. Average hardness data of 10 indentations are reported with a standard deviation.

2.5.2 Tensile Test

Flat tensile specimens (Figure 2.7) of gauge length of 15 mm, gauge width of 5 mm, overall length of 50 mm and thickness of 2 mm are cut using electro-discharge machine according to ASTM E8-04 [108].

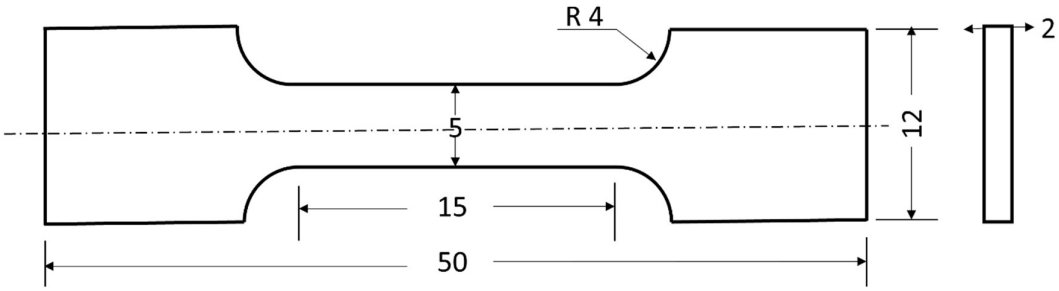

Figure 2.7: Tensile specimen with dimensions according to ASTM E8-04.

The gauge length section of the specimens is mechanically ground and polished to ensure a smooth surface without any visible cracks. Polished samples are tensile tested uniaxially at room temperature using an Instron model 5982 universal testing machine with a capacity of 100 kN. The tests are performed at a constant crosshead speed of 1 mm/min with an initial strain rate of 0.001 s^{-1}. Yield strength (YS), ultimate tensile strength (UTS), total plastic elongation, product of strength and ductility (PSE) and specific strength values are calculated from the load-elongation data and the reported values represent the average of two tests for consistency.

Work hardening rate vs true plastic strain up to ultimate tensile strength was plotted from experimental data. Logarithmic true stress vs logarithmic true plastic strain data are also calculated up to UTS for each material and were fitted using Levenberg-Marquardt iteration algorithms in Origin Pro software with Hollomon [109], Ludwik [110], Swift

[111], Ludwigson [112], and Voce [113] models described by Equations 2.11 to 2.15 to know the coefficient of strength (k) and work hardening exponent (n).

Hollomon flow model given by Equation 2.11 describes the work hardening behaviour in the uniform strain regime. Hollomon equation is valid only when the n value is equal to the uniform strain (ε_u) [114]. Most of the low carbon steels follow Hollomon equation type of flow behaviour.

$$\sigma = K\varepsilon^n \quad [2.11]$$

where K is the strength coefficient, n is the strain-hardening exponent.

Ludwik flow model given by Equation 2.12 describes the work hardening behaviour of materials with varied yield strength with similar work hardening or similar yield strength with varied work hardening. It is a modified Hollomon equation with an introduction of additional stress term (σ_0).

$$\sigma = \sigma_0 + K\varepsilon^n \quad [2.12]$$

Where σ_0 is the yield stress.

Swift flow model given by Equation 2.13 describes the work hardening behaviour of pre-strained material, with an introduction of pre-strain term to Hollomon flow model.

$$\sigma = K\,(\varepsilon_0 + \varepsilon)^n \quad [2.13]$$

Where ε_0 is pre-strain of material.

Ludwigson flow model is a modified version of Ludwik equation as given in Equation 2.14, which accounts the deviations at low strains typically occurs in case of stable austenitic stainless steels and other FCC materials with low stacking fault energies by introducing additional terms as described.

$$\sigma = K\varepsilon^n + \exp\,(K1 + n1.\varepsilon) \quad [2.14]$$

Where $K1$ and n1 were, another set of strength coefficient and strain hardening exponent at low strain.

Voce flow model describes the work hardening behaviour of materials at high stress/strain, with a saturation in stress and is given as Equation 2.15.

$$\sigma = \sigma_s - (\sigma_s - \sigma_i)\exp(n\varepsilon) \quad [2.15]$$

Where σ_s is the saturation stress, and σ_i is the true plastic stress (yield).

The best fit is judged by the high R^2 (coefficient of determination) and low χ^2 (sum of squares of deviation of calculated stress values from experimental stress values).

2.5.3 Fractography

Tensile fractured surfaces are subjected to ultrasonic cleaning to eliminate surface contaminants and studied in scanning electron microscopy (SEM) (Carl Zeiss, EVO MA15/18) to analyse the fracture mechanisms. The areal fraction analysis is carried out using ImageJ software. The percentage of dimples is obtained by taking the ratio of the total area of all dimples to the total area of the fractographs using ImageJ software after calibration of the image.

2.5.4 Elastic modulus measurement

Elastic modulus is determined using an Olympus EPOCH 600 ultrasonic tester. Initially, ultrasonic waves are transmitted through the thickness of the sample, and the velocities of the longitudinal (V_L) and transverse (V_T) waves are measured. The velocities of both waves are obtained as the average of three measurements. Poisson's ratio (υ), Elastic modulus (E), and Shear modulus (G) [115] are calculated based on these velocities and density (ρ) of materials using Equations 2.16 – 2.18.

$$\upsilon = \frac{1 - 2.\left(\frac{V_T}{V_L}\right)^2}{2 - 2.\left(\frac{V_T}{V_L}\right)^2} \quad [2.16]$$

$$E = V_L^2 . \frac{\rho.(1+\upsilon).(1-2\upsilon)}{(1-\upsilon)} \quad [2.17]$$

$$G = V_T^2 . \rho \quad [2.18]$$